



This is the accepted manuscript made available via CHORUS. The article has been published as:

## Quantum depinning of the magnetic vortex core in micron-size permalloy disks

Ricardo Zarzuela, Saül Vélez, Joan Manel Hernandez, Javier Tejada, and Valentyn Novosad

Phys. Rev. B **85**, 180401 — Published 3 May 2012

DOI: [10.1103/PhysRevB.85.180401](https://doi.org/10.1103/PhysRevB.85.180401)

# Quantum depinning of the magnetic vortex core in micron-size permalloy disks

Ricardo Zarzuela,<sup>1</sup> Saül Vézé,<sup>1</sup> Joan Manel Hernandez,<sup>1</sup> Javier Tejada,<sup>1,\*</sup> and Valentyn Novosad<sup>2</sup>

<sup>1</sup>*Grup de Magnetisme, Departament de Física Fonamental,  
Universitat de Barcelona, Barcelona 08028, Spain*

<sup>2</sup>*Materials Sciences Division, Argonne National Laboratory, Argonne, Illinois 60439, USA*

(Dated: April 16, 2012)

The vortex state, characterized by an in-plane closed flux domain structure and an out-of-plane magnetization at its centre (the vortex core), is one of the magnetic equilibria of thin soft ferromagnetic micron-size dots. In the last two decades many groups have been working on the dynamics of the magnetic moment in nanomagnetic materials at low temperatures, it giving rise to the observation of quantum relaxations and quantum hysteresis cycles. For the first time, we report experimental evidence of quantum dynamics of the vortex core of micron-size permalloy ( $\text{Fe}_{19}\text{Ni}_{81}$ ) disks induced by the application of an in-plane magnetic field. It is attributed to the quantum tunneling of the vortex core through pinning barriers, which are associated to structural defects in the dots, towards its equilibrium position.

PACS numbers: 75.45+j, 75.70Kw, 75.78Fg

In the absence of applied magnetic field, micron-size disks of soft ferromagnetic materials exhibit the vortex state as the magnetic equilibrium of the system<sup>1-3</sup>. Several technological and biomedical applications of this state have been explored, such as nonvolatile memory devices<sup>4</sup>, biomolecular carriers<sup>5</sup> and targeted cancer-cell destruction<sup>6</sup>. The vortex state is characterized by a curling magnetization and an out-of-plane magnetic core, whose size is comparable to the material's exchange length ( $\sim 6$  nm). Striking feature is the vortex core entirely governing the low frequency spin dynamics: the excitation spectrum of these micron-size disks is characterized by the *gyrotropic mode*, corresponding to the spiral-like precessional motion of the vortex core as a whole<sup>7,8</sup>.

The vortex core is a suitable candidate to observe macroscopic quantum phenomena. Because of the strong exchange interaction it behaves as an independent entity and, the vortex core being a nanoscopic object, it is feasible that it exhibits quantum tunneling between classically stable configurations. The measurement of time relaxations of the magnetic moment is a simple way to observe this phenomenon. At finite temperature these relaxations may occur via thermal activation, whereas in the limit  $T \rightarrow 0$  these relaxations continue independently of the temperature due to underbarrier quantum tunneling. Macroscopic quantum tunneling<sup>9</sup> (MQT) determines that the relaxation rate decreases as  $\exp(-S_{eff})$ , with  $S_{eff}$  the total action (including dissipation) evaluated at the magnetic thermion for a given temperature. This behaviour has been widely observed in a large number of systems<sup>10</sup>, which include single domain particles<sup>11,12</sup>, magnetic clusters<sup>13</sup>, magnetic domain walls<sup>14</sup>, flux lines in type-II superconductors<sup>15</sup> and, very recently, Normal-Superconducting interfaces in type-I superconductors<sup>16</sup>. All these experimental evidences suggest that magnetic tunneling is a common phenomenon characterizing the low-temperature dynamics of magnetic materials in the mesoscopic scale.

The application of an in-plane magnetic field yields the displacement of the vortex core perpendicularly to the field direction<sup>2</sup> (see Fig. 1b). It has been previously reported that the dynamics of the vortex core can be affected by the presence of structural defects in the sample<sup>17,18</sup>. In the present letter we explore the magnetic irreversibility and the dynamics of vortex cores in micron-size permalloy dot arrays at low temperatures by means of the application of an in-plane magnetic field. For the first time, we report experimental evidence of the quantum depinning of magnetic vortex cores.

All measurements were performed in a commercial SQUID magnetometer capable to measure at temperatures down to 2K and to apply magnetic fields up to 5T. The system is equipped with a Continuous Low Temperature Control (CLTC) and an Enhanced Thermometry Control (ETC) and it showed thermal stability better than 0.01 K at all times in any isothermal measurement. We have studied an array of permalloy disks with diameter  $2R = 1.5 \mu\text{m}$  and thickness  $L = 95$  nm. Its surface density is  $0.15$  dots/ $\mu\text{m}^2$ . Fig. 1a shows an AFM image of this array, the perspective being at 45 degrees. The array of permalloy disks was fabricated on a silicon wafer using optical lithography, and lift-off techniques: A single layer resist spin coating and highly directional electron-beam evaporation under UHV conditions were used to obtain circular dots with sharp edges. Identical properties of magnetic material, such as grain size, distribution, orientation, and film thickness may be obtained over the whole array. The magnetic film was deposited on a water-cooled substrate from a permalloy ( $\text{Fe}_{19}\text{Ni}_{81}$ ) target. The growth ratio was of  $1.5 \text{ \AA/s}$ . The 95 nm Py film showed a switching field of about 4 Oe and appeared to be pretty isotropic (in-plane). Finally, the sample was prepared by stacking four  $5 \times 5 \text{ mm}^2$  of these arrays with parallel sides and all magnetic measurements were performed using an in-plane configuration for the applied magnetic field. The sample was studied in the range of temperatures 2–300 K and under applied magnetic fields

up to 2 kOe.

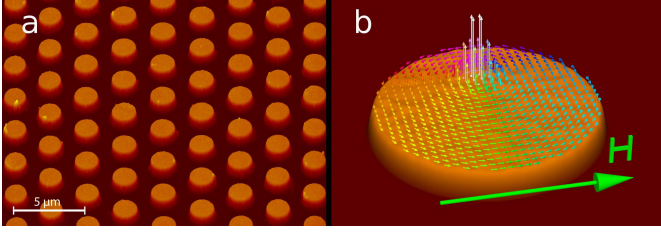


FIG. 1: **a**, AFM image of the array of permalloy disks studied. The angle of the perspective view is 45 degrees. **b**, Spin field of the vortex state in one of the permalloy disk considered in **a**. The vortex core is displaced transversely to the direction of the applied field  $H$ .

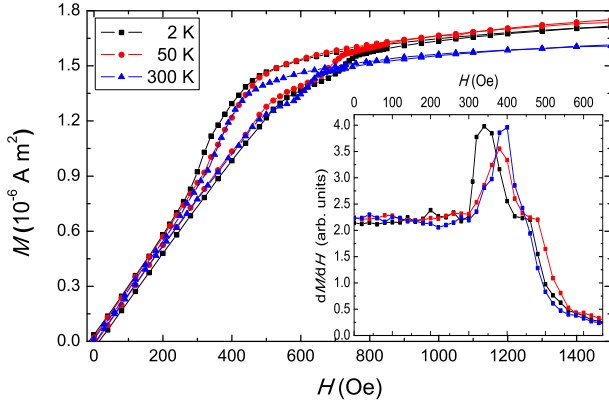


FIG. 2:  $M(H)$  loops obtained at different temperatures (2, 50 and 300 K) for the range of positive applied magnetic fields. The size of the points is bigger than the error bars. The inset shows their numerical derivative  $dM/dH$  along the descending branch.

Fig. 2 shows the  $M(H)$  curves in the range of positive applied magnetic fields, at different temperatures. For the negative range, the cycles are antisymmetric. The first magnetization curves have been omitted. Notice that these hysteresis loops correspond to the single domain (SD)  $\leftrightarrow$  Vortex transitions<sup>1,3</sup>. As the temperature is lowered, the nucleation field  $H_n$  decreases and the annihilation field  $H_{an}$  increases (as reported in Ref. 19). For the range of temperatures explored, the vortex linear regime in the descending branch should extend from 300 Oe to  $-500$  Oe at least. This has been confirmed studying the numerical derivative of the dc hysteresis loop and measuring the corresponding ac susceptibility for comparison, a method introduced in Ref. 20. Inset of Fig. 2 shows the numerical derivative  $dM/dH$  of these loops along the descending branch for positive applied magnetic fields. Notice the plateau in these derivatives for the field range 0 – 300 Oe, which is a characteristic feature of the linear regime. The ac susceptibility measurements showed a similar behavior to the one depicted in Ref. 20. On the other hand, the descending and ascend-

ing branches do not overlap at any temperature over the whole linear regime. Furthermore, the remanent magnetization increases when  $T$  decreases<sup>17</sup>. In conclusion, the vortex linear regime exhibits magnetic irreversibility and it is temperature dependent. Consequently, we proceed to explore the metastability of vortices by means of i) ZFC-FC curves ( $M_{ZFC}$  and  $M_{FC}$ ) at different magnetic fields, and ii) isothermal measurements of the magnetization along the descending branch of the hysteresis cycle ( $M_{des}(H)$ ), from the SD state, at different  $T$ . In both i) and ii) the values of  $T$  and  $H$  at which the magnetization has been measured were the same.

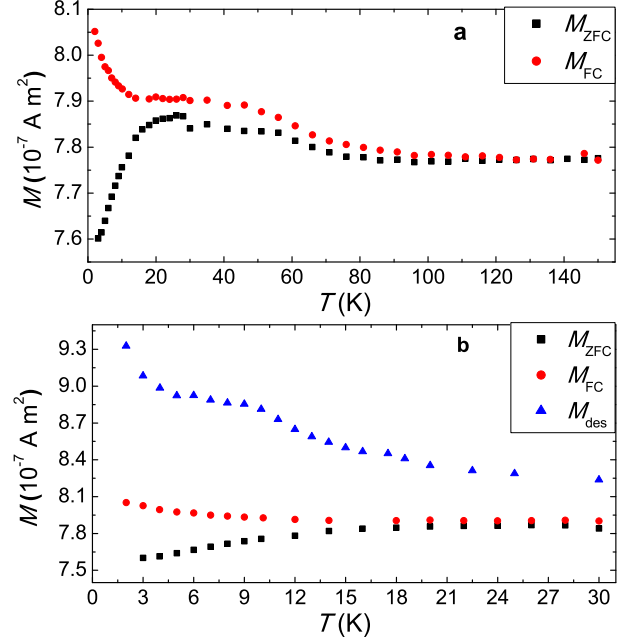


FIG. 3: **a**, Temperature dependence of  $M_{ZFC}$  (300 Oe) and  $M_{FC}$  (300 Oe) in the range 2 – 150 K. **b**, Plot of  $M_{des}$  (300 Oe), together with  $M_{ZFC}$  (300 Oe) and  $M_{FC}$  (300 Oe), in the range 2 – 30 K. See text for details.

The ZFC process consists of first performing minor cycles around  $H = 0$  Oe at  $T = 150$  K (in order to get a zero magnetization state at  $H = 0$  Oe). Secondly, the sample was cooled down to  $T = 2$  K without applied magnetic field and, thirdly, a desired magnetic field,  $H$ , was applied. Then, the ZFC magnetization curve was measured from 2 K to 150 K. Sweeping back the temperature to 2 K we follow the FC curve. Fig. 3a shows the ZFC-FC curves obtained at  $H = 300$  Oe. The magnetization increases strongly from an initial value at 2 K to a maximum in the ballpark of  $T \sim 30$  K. Then it decreases smoothly and reaches a plateau. The dependence of the FC curve on  $T$  is similar to that of the ZFC case at high temperatures but with slightly higher values of  $M$ . In the ballpark of  $T \sim 20$  K, the magnetization of the FC rises strongly, reaching its maximum value at  $T = 2$  K. This temperature dependence of both  $M_{ZFC}(H)$  and  $M_{FC}(H)$  is characteristic of the range of applied mag-

netic fields in the linear vortex regime. Additionally, isothermal magnetic measurements along the descending branch of the hysteresis cycle ( $M_{des}(H)$ ) have been measured: first, we fixed the temperature  $T$  and then we saturated the sample to the SD state by applying  $H = 1$  kOe. Secondly, we swept the magnetic field to a desired value, following the descending branch  $M_{des}$ , and finally we measured the magnetization. In both protocols we took measurements at the same values of  $T$ . Fig. 3b shows  $M_{des}(300 \text{ Oe})$  obtained in the range 2 – 30 K, together with  $M_{ZFC}(300 \text{ Oe})$  and  $M_{FC}(300 \text{ Oe})$ . The values of  $M_{des}(300 \text{ Oe})$  decrease strongly when  $T$  increases in the range 2 – 20 K and above  $T \sim 30 \text{ K}$  tend smoothly to the FC curve (not shown). The divergence between the  $M_{ZFC}$ ,  $M_{FC}$  and  $M_{des}$  curves in the range  $T = 2 - 20 \text{ K}$  indicates the existence of a strong magnetic irreversibility in this region, and therefore we will focus on this range from now on.

In order to confirm that the FC curve is the magnetic equilibria of the system, we performed two sets of measurements of the isothermal time evolution of the magnetization,  $M(T, t)$ , when sweeping the temperature in increments of 1 K per 30 minutes, a) from 15 K to 2 K and b) from 2 K to 15 K (see Ref. 21). The initial magnetic state for each set was prepared by means of the above ZFC process to the desired temperature, followed by the application of a magnetic field  $H = 300 \text{ Oe}$ . In a) it is only observed magnetic relaxation of the sample at 15 and 14 K, which quickly reaches a stable value corresponding to the FC one. From this point on, sweeping the temperature down to 2 K only leads to a variation of the magnetization of the sample following the values of the FC curve. b) shows that, in the whole range of temperatures, the magnetization relaxes. The initial value of each relaxation follows the time evolution of the previous one. Moreover, the amount of relaxed magnetization is approximately the same for  $T = 2 - 9 \text{ K}$  and it decreases progressively for 10 – 15 K with magnetization values tending to the FC ones.

We explored the metastability of the system more deeply by performing relaxation measurements in the vortex linear regime. The amount of magnetization available for relaxation is  $M_0 - M_{eq}$ , where  $M_0$  is the initial magnetization value and  $M_{eq}$  corresponds to the equilibrium magnetization. On account of this (see Fig. 3b), we will focus our study on the relaxation measurements of vortices from the metastable states of the descending branch. Fig. 4a shows the normalized irreversible magnetization (left term of equation (1)) vs.  $\ln t$  curves measured for two different applied fields ( $H = 0$  and 300 Oe) at the same temperature ( $T = 2 \text{ K}$ ). Only below  $T \sim 15 \text{ K}$  the magnetization of the sample fits very well a logarithmic time dependence. In this range of temperatures, the magnetic viscosity  $S(T)$  of the sample can be calculated by means of the theoretical formula<sup>10</sup>

$$\frac{M(t) - M_{eq}}{M_0 - M_{eq}} = 1 - S(T) \ln t \quad (1)$$

Fig. 4b shows the viscosity, as a function of  $T$ , for two different magnetic fields. In both curves we observe a plateau at low temperatures and, what is more important, it does not extrapolate to zero in the limit  $T \rightarrow 0$ . In the ballpark of  $T \sim 7 \text{ K}$ , the viscosity increases up to the temperature  $\sim 11 \text{ K}$ , from which it decreases. Relaxation measurements from the ZFC curve with different applied magnetic fields were also performed, obtaining similar results for the viscosity.

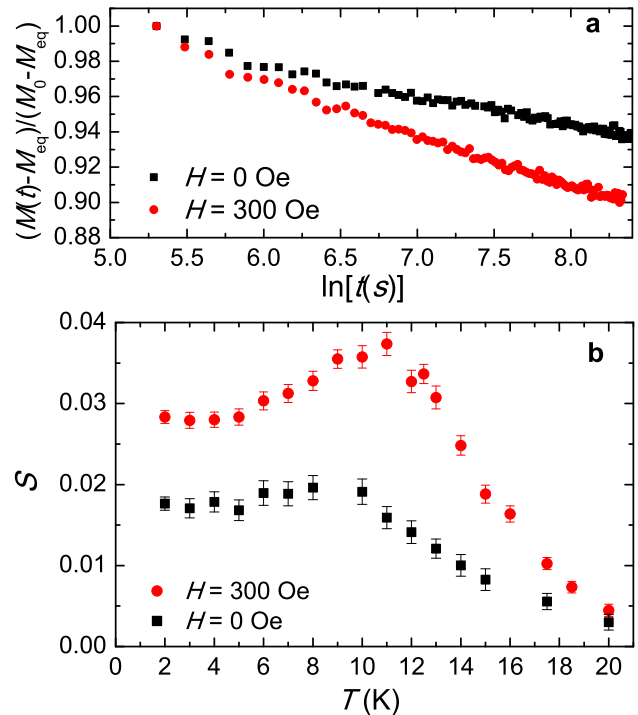


FIG. 4: **a**, Normalized irreversible magnetization vs.  $\ln t$  curves measured at  $T = 2 \text{ K}$  for  $H = 0 \text{ Oe}$  and  $300 \text{ Oe}$ . **b**, Temperature dependence of the magnetic viscosity  $S(T)$  at  $H = 0 \text{ Oe}$  and  $300 \text{ Oe}$ . See text for details.

A logarithmic time dependence of the magnetization in relaxation measurements indicates the existence of a broad distribution of energy barriers  $U$  in our system. Classically, these energy barriers can be overcome by thermal activation, whose probability is proportional to the Arrhenius factor  $\exp(-U/T)$ . The so-called Blocking temperature,  $T_B$ , sets apart both reversible ( $T > T_B$ ) and irreversible ( $T < T_B$ ) regimes when the sample is externally perturbed. Despite the slight differences between  $M_{ZFC}$  and  $M_{FC}$  and between  $M_{des}$  and  $M_{FC}$  at high temperatures, the strong divergence of magnetization observed in these curves suggests that the Blocking temperature should be below  $T \sim 20 \text{ K}$ .

Conventionally, the Blocking temperature for weakly interacting systems can be estimated as the temperature at which the magnetic viscosity reaches its maximum<sup>10</sup>. From our data  $T_B \sim 11 \text{ K}$ , which is in good agreement with the gradual loss of logarithmic time dependence of our relaxation measurements at  $T \gtrsim 15 \text{ K}$ . Notice that

thermal activation of energy barriers dies out in the limit  $T \rightarrow 0$ . Therefore, our observation that magnetic viscosity  $S(T)$  tends to a finite value different from zero as  $T \rightarrow 0$  indicates that relaxations are non-thermal in this regime, i.e., transitions from metastable states are due to underbarrier quantum tunneling. This interpretation is upheld by the  $M$  vs.  $T \ln(t/\tau_0)$  graphic representation<sup>12</sup>. The time  $\tau_0$  is the so called characteristic time attempt of the system and we have estimated its value to be<sup>22</sup>  $\tau_0 \sim 10^{-11}$ s, so that all magnetic relaxation curves only scale for temperatures above  $T_c \sim 9$  K (see Fig. 5). This loss of scaling corresponds to the quantum regime case and is independent of the energy barrier distribution. The increase of the viscosity between  $T_c$  and  $T_B$  corresponds to the thermal overcoming of the pinning energy barrier (thermal regime). Above  $T_B$ , the decrease of the viscosity when increasing the temperature corresponds to the fact there is a lower number of magnetic vortex cores in metastable states that should relax to the equilibrium magnetization, that is, magnetic irreversibility decreases with temperature.

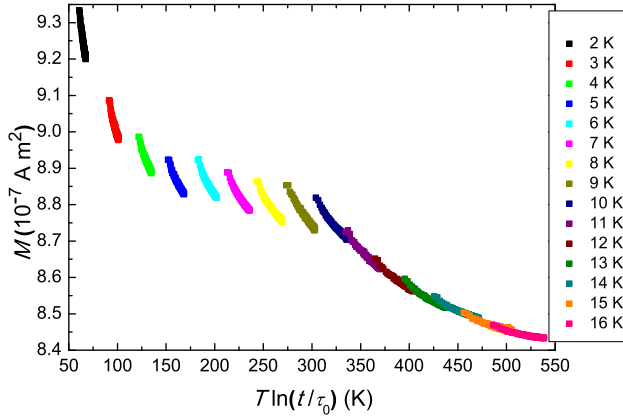


FIG. 5: Magnetization vs.  $T \ln t$  curve measured at  $H = 300$  Oe. Above  $T \sim 9$  K, we verify the scaling  $M = M(T \ln(t/\tau_0))$ , which corresponds to the case of thermal relaxation. Below  $T \sim 9$  K we find a breakdown of this scaling, which corresponds to the quantum regime case.

The onset of irreversibility appears sweeping the external magnetic field for both the ZFC curve and the descending branch. The effect of this field is to move the vortex core along the disk surface and the observed irreversibility should come from this movement. Recent experimental data report the existence of some sort of structural defects in the disks<sup>18</sup>, which could be a feasible origin of the energy barriers responsible for the magnetic dynamics of the system. In the light of this, we consider these defects are capable of pinning the vortex core. Therefore, the relaxation of the sample could be understood as simply the dynamics of the vortex core when escaping from the pinning centers towards the equilibrium.

The vortex core is described as a zero-dimensional object whose dynamics is ruled by Thiele's equation<sup>7</sup>. The

corresponding Lagrangian is given by  $\mathcal{L} = Gy\dot{x} - W(\mathbf{r})$ , where  $\mathbf{r} = (x, y)$  are the coordinates of the vortex core in the  $XY$  plane,  $G$  is the modulus of its gyrovector and  $W(\mathbf{r})$  is the total magnetic energy of the system. To incorporate the smallest pinning barriers into the model we treat the vortex core as a stack of pancake vortices, one in each atomic layer. This pancake structure shows a finite rigidity in the vertical dimension, which means that these layers interact elastically among them. We consider that just a small vertical segment of the vortex core takes part in the tunneling through the pinning barrier, whose length is  $l \ll L$ . Finally, we model the vortex core as it being a flexible line that goes predominantly along the  $\hat{z}$  direction, so that  $\mathbf{r} = \mathbf{r}(z, t)$  is a field depending on the vertical coordinate of the vortex core,  $z$ . The whole magnetic energy (including the elastic and the pinning potential) is described via<sup>23</sup>  $W(\mathbf{r}) = -\mu h x + \frac{1}{2}\kappa(x^2 + y^2) - \frac{1}{4}\beta x^4 + \frac{\lambda}{2}(\frac{\partial \mathbf{r}}{\partial z})^2$ , where  $\mu$  and  $h$  are the magnetic moment of the dot, respectively the modulus of external magnetic field (which is applied in the  $\hat{y}$  direction),  $\lambda$  is the elastic coefficient of the pancake structure and  $\kappa$  and  $\beta$  are the parameters of the potential energy. Within the framework of the Caldeira-Leggett theory<sup>9</sup>, and from the above lagrangian, the depinning exponent becomes<sup>23</sup>

$$S_{eff}(T, \epsilon) = \frac{1}{20\sqrt{2}} \frac{\kappa G}{\hbar\beta} \int d\bar{z} \oint d\bar{\tau} \left[ \frac{1}{2}\dot{u}^2 + \frac{1}{2}(u')^2 + V(u, \epsilon) \right. \\ \left. + \frac{\eta}{2\sqrt{2}\pi G} \int_{\mathbb{R}} d\bar{\tau}_1 \frac{(u(\bar{z}, \bar{\tau}) - u(\bar{z}, \bar{\tau}_1))^2}{(\bar{\tau} - \bar{\tau}_1)^2} \right] \quad (2)$$

where  $\bar{\tau}$ ,  $\bar{z}$  are dimensionless imaginary time and space coordinate respectively,  $\eta$  is the dissipative constant,  $V(u, \epsilon) = -\epsilon u + u^2 - \frac{u^4}{4}$  is the normalized energy potential,  $\epsilon = 2\sqrt{2\beta/\kappa^3}\mu h$  and  $u$  is the thermion solution of the tunneling process. Assuming a second order transition for thermal to quantum relaxation, the crossover temperature  $T_c$  can be calculated from the depinning exponent by means of Ginzburg-Landau's theory for second order phase transitions<sup>24</sup>. In absence of applied magnetic field ( $h = 0$ )  $T_c$  and the height of the barrier  $U$  become<sup>23</sup>

$$k_B T_c \simeq \sqrt{5} \frac{\hbar\kappa}{2\pi G}, \quad U = \frac{\kappa^2}{4\beta} \quad (3)$$

where the modulus of the gyrovector is given by the formula  $G = 2\pi(+1)IM_s/\gamma$ , so that it is related to the tunneling vertical segment.

Comparison of the theoretical model with the experimental results leads to the determination of the parameters  $(\kappa, \beta)$ : first of all, notice that  $l$  cannot be smaller than the material's exchange length because, otherwise, the deformation of the vortex core line would be energetically unfavorable to the system. The same happens if  $l$  is much bigger than this exchange length. So it should be  $l \sim l_{ex} = \sqrt{2A/\mu_0 M_s^2} \simeq 6$  nm, where  $A = 1.3 \cdot 10^{-11}$

$J/m$  is the exchange constant and  $M_s = 7.5 \cdot 10^5$  A/m is the saturation magnetization of permalloy. The value of the modulus of the gyrovecton is  $G = 2\pi(+1)lM_s/\gamma = 1.62 \cdot 10^{-13}$  Ns/m ( $\gamma = 1.76 \cdot 10^{11}$  (Ts) $^{-1}$ ). Experimentally, we have  $T_c \sim 9$  K for the  $H = 0$  Oe case too, from which we deduce the value  $\kappa \sim 0.5$  J/m $^2$ . On the other hand, for a measurable tunneling rate  $S_{eff}$  should be in the ballpark of 30. As  $S_{eff} = c\kappa G/2\sqrt{2}\hbar\beta$  with  $c$  being a numerical factor of order unity resulting from the integration, we have the following estimate of the coefficient  $\beta$ ,  $\beta \sim \kappa G/60\sqrt{2}\hbar = 9.8 \cdot 10^{18}$  J/m $^4$ . Finally, from these values we can estimate the width of the energy barrier, which is given by the expression  $L_B = \sqrt{2\kappa/\beta} \sim 0.3$  nm. Furthermore, we can also estimate the order of magnitude of the height of the barrier (mean value),  $U \sim 250$  K, which is in good agreement with the value given by the Blocking temperature. These estimates are feasible values because pinning happens at the atomic level.

In conclusion, non-thermal dynamics of magnetic vortices in micron-size permalloy disks is reported. It is attributed to the quantum depinning of vortex cores through the structural defects of the sample, in steps about 0.3 nm.

R.Z. and S.V. acknowledge financial support from the Ministerio de Ciencia e Innovación de España. J.T. acknowledges financial support from ICREA Academia. The work at the University of Barcelona was funded by the Spanish Government Project No. MAT2008-04535. The work at Argonne National Laboratory, including the use of facility at the Center for Nanoscale Materials (CNM), was supported by UChicago Argonne, LLC, Operator of Argonne National Laboratory ("Argonne"). Argonne, a U.S. Department of Energy Office of Science Laboratory, is operated under Contract No. DE-AC02-06CH11357.

- 
- \* Electronic address: [jtejada@ubxlab.com](mailto:jtejada@ubxlab.com)
- <sup>1</sup> R. P. Cowburn, D. K. Koltsov, A. O. Adeyeye, M. E. Welland, and D. M. Tricker, *Phys. Rev. Lett.* **83**, 1042 (1999).
  - <sup>2</sup> T. Shinjo, T. Okuno, R. Hassdorf, K. Shigeto, and T. Ono, *Science* **289**, 930 (2000).
  - <sup>3</sup> V. Novosad *et al.*, *Phys. Rev. B* **65**, 060402 (2002).
  - <sup>4</sup> S. S. P. Parkin, M. Hayashi, and L. Thomas, *Science* **320**, 190 (2008).
  - <sup>5</sup> E. A. Rozhkova *et al.*, *J. Appl. Phys.* **105**, 07B306 (2009).
  - <sup>6</sup> D.-H. Kim *et al.*, *Nature Materials* **9**, 165 (2010).
  - <sup>7</sup> K. Yu. Guslienko *et al.*, *J. Appl. Phys.* **91**, 8037 (2002).
  - <sup>8</sup> S.-B. Choe *et al.*, *Science* **304**, 420 (2004).
  - <sup>9</sup> A. O. Caldeira and A. J. Leggett, *Phys. Rev. Lett* **46**, 211 (1981). A. O. Caldeira and A. J. Leggett, *Ann. Phys. (N.Y.)* **149**, 374 (1983).
  - <sup>10</sup> E.M. Chudnovsky and J. Tejada, *Macroscopic Quantum Tunneling of the Magnetic Moment* (Cambridge University Press, Cambridge, 1998).
  - <sup>11</sup> J. Tejada and X. X. Zhang, *J. Magn. Magn. Mater.* **140-144**, 1815 (1995). R. Sappey, E. Vincent, M. Ocio, and J. Hammann, *J. Mag. Mag. Mat.* **221**, 87 (2000). D. D. Awschalom, J. F. Smyth, G. Grinstein, D. T. DiVincenzo, and D. Loss, *Phys. Rev. Lett.* **68**, 3092 (1992).
  - <sup>12</sup> E. Vincent, J. Hammann, P. Prené, and E. Tronc, *J. Phys. I France* **4**, 273 (1994).
  - <sup>13</sup> Jonathan R. Friedman, M. P. Sarachik, J. Tejada, and R. Ziolo, *Phys. Rev. Lett.* **76**, 3830 (1996). J. M. Hernandez *et al.*, *Phys. Rev. B* **55**, 5858 (1997).
  - <sup>14</sup> J. Brooke, T. F. Rosenbaum, and G. Aeppli, *Nature* **413**, 610 (2001).
  - <sup>15</sup> A. Hamzic, L. Fruchter, and I. A. Campbell, *Nature (London)* **345**, 515 (1990). J. Tejada, E. M. Chudnovsky and A. García, *Phys. Rev. B* **47**, 11552 (1993).
  - <sup>16</sup> E. M. Chudnovsky, S. Vélez, A. García-Santiago, J. M. Hernandez, and J. Tejada, *Phys. Rev. B* **83**, 064507 (2011); R. Zarzuela, E. M. Chudnovsky and J. Tejada, *Phys. Rev. B* **84**, 184525 (2011).
  - <sup>17</sup> H. Shima *et al.*, *J. Appl. Phys.* **92**, 1473 (2002).
  - <sup>18</sup> R.L. Compton, T. Y. Chen, and P. A. Crowell, *Phys. Rev. B* **81**, 144412 (2010).
  - <sup>19</sup> G. Mihajlovic *et al.*, *Appl. Phys. Lett.* **96**, 112501 (2010).
  - <sup>20</sup> J. A. J. Burgess *et al.*, *Phys. Rev. B* **82**, 144403 (2010).
  - <sup>21</sup> See Supplemental Material for supplemental data.
  - <sup>22</sup> The value of  $\tau_0$  is such that the magnetization  $M$  of a relaxation process scales with  $T \ln(t/\tau_0)$  in the thermal regime. The protocol to find  $\tau_0$  consists of plotting  $M(T \ln(t/\tau_0))$  for different values of  $\tau_0$ , which are powers of 10 because only its order of magnitude is relevant to the relaxation process (see Ref. 10). Then the value of  $\tau_0$  corresponds to the best scaling of the resulting  $M(T \ln(t/\tau_0))$  plots.
  - <sup>23</sup> R. Zarzuela, J. M. Hernandez and J. Tejada. To be submitted.
  - <sup>24</sup> I. Affieck, *Phys. Rev. Lett.* **46**, 388 (1981); A. I. Larkin and Yu. N. Ovchinnikov, *Pis'ma Zh. Eksp. Teor. Fiz.* **37**, 322 (1983) [*JETP* **37**, 382 (1983)]; E. M. Chudnovsky, *Phys. Rev. A* **46**, 8011 (1992).